Published in final edited form as:

Adv Healthc Mater. 2018 May ; 7(10): e1701469. doi:10.1002/adhm.201701469.

Injectable, Tough Alginate Cryogels as Cancer Vaccines

Ting-Yu Shih,
John A. Paulson School of Engineering and Applied Sciences, Harvard University, Cambridge, MA 02138, USA; Wyss Institute for Biologically Inspired Engineering at Harvard University, Boston, MA 02115, USA

Serena O. Blacklow,
John A. Paulson School of Engineering and Applied Sciences, Harvard University, Cambridge, MA 02138, USA

Dr. Aileen W. Li,
John A. Paulson School of Engineering and Applied Sciences, Harvard University, Cambridge, MA 02138, USA; Wyss Institute for Biologically Inspired Engineering at Harvard University, Boston, MA 02115, USA

Dr. Benjamin R. Freedman,
John A. Paulson School of Engineering and Applied Sciences, Harvard University, Cambridge, MA 02138, USA; Wyss Institute for Biologically Inspired Engineering at Harvard University, Boston, MA 02115, USA

Dr. Sidi Bencherif,
John A. Paulson School of Engineering and Applied Sciences, Harvard University, Cambridge, MA 02138, USA; Wyss Institute for Biologically Inspired Engineering at Harvard University, Boston, MA 02115, USA; Laboratory of Biomechanics & Bioengineering (BMBI) UMR CNRS 7388, Sorbonne University, University of Technology of Compiègne (UTC), 60200 Compiègne, France; Department of Chemical Engineering, Northeastern University, Boston, MA 02115, USA

Dr. Sandeep T. Koshy,
John A. Paulson School of Engineering and Applied Sciences, Harvard University, Cambridge, MA 02138, USA; Wyss Institute for Biologically Inspired Engineering at Harvard University, Boston, MA 02115, USA; Harvard-MIT Division of Health Sciences and Technology, Cambridge, MA 02139, USA

Dr. Max C. Darnell, and
John A. Paulson School of Engineering and Applied Sciences, Harvard University, Cambridge, MA 02138, USA; Wyss Institute for Biologically Inspired Engineering at Harvard University, Boston, MA 02115, USA

Prof. David J. Mooney[*]

[*] mooneyd@seas.harvard.edu.

Supporting Information

Supporting Information is available from the Wiley Online Library or from the author.

John A. Paulson School of Engineering and Applied Sciences, Harvard University, Cambridge, MA 02138, USA; Wyss Institute for Biologically Inspired Engineering at Harvard University, Boston, MA 02115, USA

Abstract

A covalently crosslinked methacrylated (MA)-alginate cryogel vaccine has been previously shown to generate a potent response against murine melanoma, but is not mechanically robust and requires a large 16G needle for delivery. Here, covalent and ionic crosslinking of cryogels were combined with the hypothesis that this would result in a tough MA-alginate cryogel with improved injectability. All tough cryogels can be injected through a smaller, 18G needle without sustaining any damage, while covalently crosslinked-only cryogels break after injection. CpG-delivering tough cryogels effectively activate dendritic cells (DCs). GM-CSF-releasing tough cryogels recruit 5 times more DCs than blank gels by Day 7 *in vivo*. The tough cryogel vaccine induces strong antigen-specific cytotoxic T-lymphocyte and humoral responses. These vaccines prevent tumor formation in 80% of mice inoculated with HER2/neu-overexpressing DD breast cancer cells. The MA-alginate tough cryogels provide a promising minimally invasive delivery platform for cancer vaccinations.

Keywords

injectable; alginate; tough cryogels; cancer vaccines

1. Introduction

Cancer vaccines have gathered significant attention recently because of their potential to eliminate tumors and establish immunological memory to prevent recurrence.[1–2] Cell-based vaccines typically involve isolating patients' own dendritic cells (DCs) or other immune cells and activating them *ex vivo*. The activated cells are then transplanted back into the patients. However, clinical success of cancer vaccines has been limited, likely due to tumor immunosuppression or short lifespan of transplanted activated cells.[3–6]

Biomaterial-based approaches to cancer vaccination have demonstrated promise in enhancing the effectiveness of cancer vaccines.[2, 7–9] In particular, scaffold-based vaccines have been shown to successfully modulate host immune cells *in situ* and evoke potent antitumor responses.[10–12] After implantation, these scaffolds release granulocyte macrophage colony-stimulating factor (GM-CSF) to attract DCs to the scaffold site. In the scaffold, DCs are activated by CpG-oligonucleotide (CpG-ODN) and tumor antigens, and then the activated DCs home to the draining lymph nodes (dLNs) and present the antigens to T cells to induce potent anti-tumor responses. A vaccine based on porous poly(lactide-co-glycolide) scaffolds is currently undergoing a Phase-I clinical trial.[13]

A covalently crosslinked methacrylated (MA)-alginate cryogel was developed to be a preformed injectable platform for cancer vaccination.[14] When the methacrylate groups on MA-alginate are crosslinked by free radical polymerization at −20°C, the crosslinking occurs around ice crystals. Thawing leads to cryogels with a macroporous structure that

allows for DC trafficking. The cryogel also has excellent deformability and shape-memory that allows minimally invasive delivery through a needle and syringe. Compared to typical injectable scaffolds that are formed *in situ* after injection, the preformed cryogels hold several advantages, including the ability to create well-defined macrostructure and microstructure following injection, maintenance of a defined volume of gel at the injection site, bypassing the need for appropriate gelling conditions *in vivo*, or and the ability to remove before injection any potentially toxic precursor and crosslinking materials that could damage the surrounding tissues.[15] The cryogel vaccine has been shown to generate effective immunity against an aggressive melanoma model in mice.[12] However, those cryogels were not mechanically robust. They required a large 16G needle for delivery, causing a large wound after injection, and can break during injection. While gel breakage is not expected to have a detrimental effect on the vaccine efficacy, the inability to precisely localize the vaccine could present logistical and regulatory issues, and it would be difficult to locate gel fragments for biopsy analysis. Furthermore, delivery through a smaller needle would allow easier subcutaneous injection into patients. While simply fabricating smaller cryogels may avoid these issues, this would limit drug loading capacity, and likely modulate a smaller number of immune cells.

In this study, we hypothesized that combining covalent and ionic crosslinking would result in a tough MA-alginate cryogel with improved injectability. Previously, a network of covalently and ionically crosslinked polymers has demonstrated strikingly high toughness in the bulk form.[16] Upon compression, the weaker ionic crosslinks will reversibly break first from the stress and dissipate energy that would have permanently broken the covalent crosslinks, thereby enhancing the toughness of the hydrogel. We fabricated a tough cryogel by incorporating ionic crosslinks to the covalently crosslinked MA-alginate cryogels via calcium ions. Alginate is a natural polymer that has been used in many biomedical applications, including drug delivery, cell delivery and tissue engineering.[17] Calcium ions are commonly used in forming alginate hydrogels, and the hydrogel mechanical properties can be varied by changing the amount of calcium ions.[17] Furthermore, calcium ions play an important role in regulating immune responses, and have been shown to promote inflammatory innate immunity and pathogen-specific humoral immunity.[18–19] The ability of tough MA-alginate cryogels to be needle-injected without sustaining damage was tested by injection via 16 and 18G needles. Antigen-specific cellular and humoral immune responses were studied to demonstrate the utility of this material to serve as a cancer vaccine platform. To explore the broad utility of the scaffold-based cancer vaccination approach, the efficacy of the tough cryogel as a prophylactic vaccine was investigated in a murine breast cancer model. Moreover, the effect of vaccine placement with respect to the dLNs was examined.

2. Results

2.1 Injection testing of cryogels

To study whether ionic crosslinking could prevent cryogels from sustaining damage during needle injection, MA-Alginate cryogels were soaked in a 200 mM $CaCl_2$ bath to introduce ionic crosslinking **(**Figure 1**)**. The cryogels were then loaded into a 16G or 18G needle

attached to a syringe and injected **(**Figure 2A**)**. Soaking times were varied to introduce different calcium concentrations to the cryogels (Figure 2B). Increasing soaking time, corresponding to increasing calcium concentration in the gel, enhanced gel toughness until the toughening effect plateaued at 10 min soaking time (37 mM calcium in the gel); all gels remained intact after injection when soaked for 10 min in the calcium bath. Longer soaking times led to a proportion of the gels sustaining damage after injection (Figure 2C). The 10-minute soaking time led to a significantly higher proportion of intact gels after injection compared to other soaking times except 5 min. The cryogels soaked in a 200 mM calcium bath for 10 min were used for all following experiments and were referred to as tough cryogels.

The ability of tough cryogels to be injected through a smaller, 18G needle (inner cross-sectional area 50% smaller than that of a 16G needle) without sustaining damage was then tested. SEM images confirmed that the tough cryogels remained intact after 18G needle injection, whereas the covalently crosslinked-only cryogels were damaged after injection (Figure 2D). All tough gels could pass through an 18G needle intact, while all covalently crosslinked-only cryogels sustained damage after injection (Figure 2E, Movie S1).

It was next determined whether tough cryogels reform and maintain their structure after subcutaneous needle injection. High frequency ultrasound (HFUS) imaging revealed that cryogel formulation was a significant factor on gel circularity and thickness post-injection **(**Figure 3A-C**)**. Tough cryogels remained more circular than covalently crosslinked-only cryogels after injection, independent of the needle gauge used for injection, with circularity similar to the theoretical circularity for a cryogel (0.74). Furthermore, tough cryogels maintained their thickness better than covalently X-linked only cryogels (actual thickness ~2.0 mm). Explantation of the cryogels confirmed that tough cryogels maintained their structure after both 16G and 18G needle injection while covalently X-linked only cryogels fractured post-injection (Figure 3D).

2.2 Structural, mechanical and swelling properties

Scanning electron microscopy (SEM) images showed that tough cryogels have a highly porous structure, which was maintained after needle injection **(**Figure 4A**)**. Macroscopically, the tough cryogel's structure was also maintained after needle injection, with no significant changes in diameter or thickness observed **(**Figure S1**)**. The interconnected porosity, pore space dimension, stiffness, and swelling ratio of tough cryogels were next characterized, in comparison to covalently crosslinked-only cryogels. The presence of calcium did not dramatically affect interconnected porosity, as tough cryogels remained highly porous even though the difference was significant compared to covalently crosslinked-only cryogels (Figure 4B). As previous work has demonstrated, DC migration is impeded when scaffold pore size falls below 75 μm,[20] the dimension distribution of the pore space in the cryogels in the hydrated state was quantified. Analyses of confocal microscopy images revealed that both types of cryogels have a similar distribution of pore space dimensions **(**Figure S2**)**. Approximately 80% of the pore space is greater than 75 μm, with median pore space at the 100 μm range for both types of cryogels. The high interconnected porosity and large pore space of tough cryogels is important to allow for immune cell trafficking. The stiffness of

the two types of cryogels was also not significantly different, indicating that tough cryogels preserve the deformability favorable for needle injection (Figure 4C). Notably, tough cryogels had a significantly smaller swelling ratio compared to covalently crosslinked-only cryogels, supporting the formation of ionic crosslinks in tough cryogels (Figure 4D).

2.3 *In vitro* DC activation

To study whether tough cryogels are inherently immune-activating, BMDCs were seeded in the tough cryogels and cultured overnight. FACS analysis showed that DCs cultured in tough cryogels had significantly upregulated CD86 expression compared to those cultured in covalently crosslinked-only cryogels **(**Figure 5A**)**.

To determine whether CpG-ODN-loaded tough cryogels can activate DCs in a sustained manner, tough cryogels were first placed in a release buffer over a period of time *in vitro*. Following an initial burst release, CpG-ODN delivered by tough cryogels displayed sustained release for at least 14 days, with approximately half of CpG-ODN remaining in the gels (Figure 5B). After releasing CpG-ODN for 3 days to 2 weeks, tough cryogels were co-cultured on a monolayer of BMDCs *in vitro* overnight. The tough cryogels delivering CpG-ODN induced significant upregulation of CD86 and MHC class II molecules on DCs even after two weeks of CpG-ODN release compared to blank tough cryogels (Figure 5C).

2.4 *In vivo* immune cell recruitment

Recruitment of DCs to the scaffold site is a critical step in vaccination in this approach. GM-CSF delivered by tough cryogels displayed sustained release *in vitro* for at least 14 days following an initial burst release **(**Figure 6A**)**. To examine the ability of tough cryogels to recruit DCs *in vivo*, blank tough cryogels or tough cryogels delivering GM-CSF were injected subcutaneously into mice. Tough cryogels delivering GM-CSF recruited five times more immune cells than blank tough cryogels (Figure 6B). More importantly, tough cryogels delivering GM-CSF recruited approximately three times more DCs than the blank cryogels (Figure 6C). Tough cryogels delivering GM-CSF also recruited a significant number of neutrophils, but fewer macrophages, compared with the blank cryogels (Figure 6D and 6E).

2.5 Antigen-specific cytotoxic T-lymphocyte and humoral responses

To determine whether the tough cryogel vaccine could elicit an antigen-specific cytotoxic T-lymphocyte (CTL) and humoral responses, mice were vaccinated against a model antigen, ovalbumin (OVA). The vaccinated mice had a significantly higher fraction of SIINFEKL tetramer$^+$ CD8 T cells as well as IFN-γ^+ CD8 T cells in blood compared to mice receiving blank tough cryogels **(**Figure 7A-B**)**. Furthermore, the vaccinated mice had significantly higher anti-OVA IgG1 and IgG2a antibody titers than mice receiving blank tough cryogels (Figure 7C-D). Altogether, these results demonstrate that the tough cryogel vaccine could generate antigen-specific CTL and humoral responses.

2.6 Anti-tumor humoral immunity and prophylactic efficacy

The ability of the tough cryogel vaccine to induce an anti-tumor response *in vivo* was tested in a prophylactic breast cancer model **(**Figure 8A**)**. Mice were either given two blank tough

cryogels as the control or vaccinated by the full tough cryogel vaccine implanted either near or far from the draining inguinal LNs (Figure 8B).

Mice vaccinated by the full vaccine generated significantly higher levels of anti-HER2/neu antibodies compared to the control mice by Day 14 (Figure 8C). High levels of anti-HER2/neu antibodies were maintained in the vaccinated mice on Day 28 and Day 37. Interestingly, mice with the vaccination site closer to the dLN had a significantly higher level of anti-HER2/neu antibodies than those with vaccination site farther from the dLN on Day 14. Both groups had similar antibody levels in the subsequent time points, indicating that vaccination closer to the dLN induces a faster humoral response.

The tough cryogel vaccine implanted close to the dLNs induced strong protective immunity against DD breast cancer cells, as 80% of the vaccinated mice remained tumor free for more than 150 days after tumor challenge. The tough cryogel vaccine implanted farther from the dLNs generated lesser protective immunity, with 40% of the vaccinated mice remaining tumor free in the same period. Mice in the vaccine groups that did develop tumors had delayed tumor onset and tumor growth, as compared to control mice which all developed tumors within 7 days of inoculation (Figure 8D). Furthermore, the vaccinated mice had significantly prolonged survival, with 80% and 40% survival (near and far from LNs, respectively) by Day 150. In contrast, all control mice had to be euthanized within approximately 80 days, with a median survival of 57 days (Figure 8E). The needle gauge used for injection did not affect survival efficacy with the tough cryogel vaccine (Figure 8F).

4. Discussion

Incorporation of ionic crosslinking into MA-alginate cryogels enhanced toughness and improved cryogel injectability. Tough cryogels can be injected both *in vitro* and *in vivo* through an 18G needle that has an inner cross-sectional area 50% smaller than a 16G needle, but covalently crosslinked-only cryogels all broke after injection through an 18G needle. Ionic crosslinks are dynamic, and provide a mechanism for energy dissipation that lowers the energy experienced by covalent crosslinks. Calcium ions only bind to the carboxyl groups from guluronate blocks (G blocks) on adjacent alginate polymer chains to form the crosslinks.[17, 21] Since methacrylation of alginate replaces carboxyl groups with methacrylate functional groups, the binding of calcium ions to G blocks is likely interrupted. However, the significant decrease in swelling ratio suggests maintenance of ionic crosslinking capacity in the tough cryogel, even though the amount of crosslinking might be lower than it would be with unmodified alginate. The decrease in swelling ratio did not lead to significant shrinkage of pore space dimensions as both tough and covalently crosslinked-only cryogels have approximately 80% of the pore space greater than 75 μm. This is likely because ionic crosslinking takes place in the gel wall, and the nanopores in the gel wall may have decreased in size. However, the large pore space that allows dendritic cell trafficking is pre-defined by the size and shape of ice crystals, and is not affected by ionic crosslinking. Interestingly, despite the additional crosslinking, tough cryogels have a similar Young's modulus compared to that of covalently crosslinked-only cryogels. This may result from both types of cryogels having similar porous structures with approximately 90% interconnected porosity. During compression testing, the deformation of the cryogels is in

large part due to the collapse of pores. This is clear from previous atomic force microscopy analysis, which revealed the local stiffness of the covalently crosslinked-only MA-alginate cryogels is ~100 MPa, approximately six orders of magnitude higher than the bulk stiffness.[22]

We observed that increasing the calcium concentration in the cryogel up to an optimal concentration improved gel injectability, while a significant proportion of the gels with higher calcium concentrations sustained damage after injection. This trend has been observed in other tough hydrogels.[16, 23–24] This phenomenon is likely because the gel becomes very stiff on the local level at high degrees of ionic crosslinking, and fewer ionic crosslinks break upon compression. The optimized tough cryogel is able to maintain both its micro- and macro-architecture after injection, as no permanent changes to its porous structure and bulk physical dimensions were observed. Therefore, viscous effects likely only have a negligible impact on the tough cryogel during its intra-needle transit, likely due to the short transit time. Since there is no enzyme in humans or animals that can degrade alginate,[17] the tough cryogel can likely remain stable *in vivo* for a long time. This, coupled with the fact that the tough cryogel preserves its structure after *in vivo* subcutaneous injection, suggest that the tough cryogel is potentially an ideal material for long-term cell modulation or drug delivery.

The tough cryogel vaccine generated strong antigen-specific CTL and humoral responses. Significantly increased percentages of SIINFEKL tetramer$^+$ and IFN-γ^+ CD8 T cells as well as anti-OVA and anti-HER2/neu antibody titers were detected in the blood of vaccinated mice. While we did not investigate the contribution of HER2/neu-specific CD8 T cells to the prophylactic efficacy in the breast cancer model, we expect the expansion of HER2/neu-specific CD8 T cells aids in preventing tumor formation. Anti-HER2/neu antibodies may also play a role in tumor protection, with different IgG subclasses having different effector functions.[25] Murine IgGl antibodies bind and directly neutralize, whereas IgG2a antibodies bind and facilitate antibody-dependent cellular cytotoxicity by effector cells such as natural killer cells or macrophages. In this study, we only quantified the pan-IgG anti-HER2/neu titer, but using OVA we demonstrated that the tough cryogel vaccine was able to generate IgGl and IgG2a subtypes. Further studying the titers of IgG subclasses and the roles they play following vaccination could provide useful information for future scaffold-based vaccine design.

Calcium in the tough cryogel stimulated DC activation *in vitro*. BMDCs cultured in the tough cryogel had significantly greater upregulation of the CD86 activation marker than those cultured in covalently crosslinked-only cryogels. It has been reported that calcium ions and calcium phosphate crystals can activate the NLRP3 inflammasome,[19, 26–28] which is part of the innate immune system that regulates the secretion of pro-inflammatory cytokines IL-1β and IL-18,[29] DCs encapsulated in calcium crosslinked alginate bulk hydrogels were previously found to secrete significantly more IL-1β *in vitro* compared to DCs encapsulated in agarose or collagen hydrogels without calcium crosslinking.[30] These same alginate hydrogels also increased IL-1β concentration in the surrounding tissue *in vivo*.[30] Understanding and harnessing the downstream immune responses resulted from calcium may enhance the anti-tumor response of tough cryogel vaccines.

Tough cryogels delivering GM-CSF recruited a significant number of neutrophils *in vivo*. Neutrophils are traditionally considered first responders to acute inflammation, killing pathogens through phagocytosis, release of pro-inflammatory proteins and deployment of neutrophil extracellular traps.[31] However, more recently neutrophils have been shown to interact with B cells and enhance IgM and IgG secretion, but suppress T cell activities.[31] How neutrophils effect vaccine efficacy and how they may be utilized in concert with adaptive immunity still needs to be explored, and likely provides another parameter to optimize the design of the tough cryogel vaccine, or scaffold-based vaccines in general.

The distance from the vaccine scaffold to the dLN was found to affect the kinetics of the antibody response. To the best of our knowledge, this is the first time this finding is documented in a scaffold-based vaccine. It is likely that the time required for DCs to traffic to the dLN is directly related to the vaccine distance from the dLN. The kinetics may not be key for a prophylactic vaccine, but a faster response may be critical for therapeutic vaccination.[32–33] The finding suggests placement of the vaccine as an important consideration for the deployment of a scaffold-based vaccine.

The tough cryogel vaccine provided strong tumor-free protection against breast cancer in a murine model. Up to 80% of vaccinated mice remained tumor free 5 months after tumor challenge. While prophylactic mastectomy is highly successful in preventing breast cancer in the clinic,[34–36] our vaccine could potentially serve as a minimally invasive, less destructive alternative. It could also be used as a combination therapy in $HER2^+$ breast cancer patients with the standard therapy, trastuzumab, to prevent recurrence. Moreover, together with the efficacy previously showed against an aggressive murine melanoma model using other scaffolds,[10, 12, 37] our results demonstrate the broad utility of scaffold-based cancer vaccines.

4. Conclusions

An injectable tough MA-alginate cryogel has been developed to serve as a cancer vaccine that can be delivered in a minimally invasive manner. Combining covalent and ionic crosslinking, the tough cryogel demonstrated superior injectability compared to covalently crosslinked-only cryogels. The tough cryogels enhanced recruitment of DCs and other immune cells. The tough cryogel vaccine generated strong antigen-specific cellular and humoral responses *in vivo*, and provided potent prophylactic efficacy against a murine breast cancer model. Furthermore, vaccination closer to the dLN induced a faster antibody response. The tough cryogels present a promising minimally invasive delivery platform for cancer vaccinations.

5. Experimental Section

Materials

LF20/40 and UP MVG sodium alginate were purchased from NovaMatrix (Sandvika, Norway). The two types of alginate have similar properties (Mw ~250 kDa, G content ~70%), except that UP MVG is a medical grade, ultrapure alginate with very low endotoxin level (≤100 EU/g). UP MVG alginate was used in all cell and animal studies, as well as pore

size characterization studies to ensure that the cryogels used in cell and animal studies have large pore sizes. LF20/40 alginate was used in the other studies. 2-(N-Morpholino) ethanesulfonic acid hydrate (MES), N-(3-Dimethylaminopropyl)-N'-ethylcarbodiimide hydrochloride (EDC), N-hydroxysuccinimide (NHS), dimethylformamide (DMF), trimethylamine (TEA), ammonium persulfate (APS), N, N, N', N'-tetram ethyl ethyl enedi amine (TEMED), anhydrous calcium chloride, HEPES, and alginate lyase were purchased from Sigma-Aldrich (Atlanta, GA). 2-aminoethyl methacrylate hydrochloride (AEMA) was purchased from Polysciences (Warrington, PA). Integrin binding peptide Gly-Gly-Gly-Gly-Arg-Gly-Asp-Ser-Pro (GGGGRGDSP) was synthesized by Peptides International (Louisville, KY). Acrylate-poly(ethylene glycol)-N-hydroxysuccinimide (ACRL-PEG-NHS) (3.5 kDa) was purchased from JenKem Technology (Beijing, China). Hexamethyldisilazane (HMDS) was purchased from Electron Microscopy Sciences (Hatfield, PA). Cyanine 5-amine (Cy5-amine) fluorescent dye was purchased from Lumiprobe (Hunt Valley, MD). Granulocyte macrophage colony-stimulating factor (GM-CSF) was purchased from PeproTech (Rocky Hill, NJ). CpG-ODN 1826 5'-tccatgacgttcctgacgtt-3' was synthesized by Integrated DNA Technologies (Chicago, IL). The Quant-it™ OliGreen® ssDNA Assay Kit was purchased from Thermo Fisher Scientific (Waltham, MA). The GM-CSF ELISA kit was purchased from R&D Systems (Minneapolis, MN). OVA was purchased from InvivoGen (InvivoGen vac-pova, San Diego, CA). RPMI 1640 media and ACK lysis buffer were purchased from Lonza (Basel, Switzerland). HER2/neu-overexpressing DD breast cancer cell line, CT26, and HER2/neu-overexpressing CT26 colon cancer cell lines were obtained from Professor Glenn Dranoff's laboratory, Dana-Farber Cancer Institute, Boston, Massachusetts.[38–39] BALB/cJ and C57BL/6J mice were purchased from the Jackson Laboratory (Bar Harbor, ME). APC-conjugated H-2Kb-SIINFEKL tetramer was obtained from the NIH tetramer core facility.

Synthesis of methacrylated alginate

MA-alginate was synthesized as described previously.[14] Briefly, LF20/40 or UP MVG sodium alginate (1.2 g) was dissolved in a 0.1 M MES buffer (pH ~6.5) at 0.6% (w/v). NHS (1.56 g) and EDC (3.36 g) were added to the alginate solution to activate the carboxyl groups of alginate. Then, AEMA (2.688 g) was added to the reaction mixture and stirred for 17 h at room temperature (RT) in the dark. The mixture was precipitated in excess acetone, filtered, and dried in a vacuum chamber at RT overnight.

Synthesis of ACRL-PEG-RGD

ACRL-PEG-GGGGRGDSP (ACRL-PEG-RGD) was synthesized by conjugating an RGD peptide to ACRL-PEG-NHS.[40] Briefly, GGGGRGDSP peptide (100 mg) was first dissolved in anhydrous DMF (30 mL) with TEA (4 M excess). Then, ACRL-PEG-NHS (419 mg) was dissolved in anhydrous DMF and immediately added to the peptide mixture (at an ACRL-PEG-NHS to peptide ratio of 1:1.1) and stirred for 3 h at RT. The reaction mixture was precipitated twice in cold anhydrous ether and dried in a vacuum chamber overnight at RT. The conjugation was confirmed by NMR (Varian Unity Inova500B, Palo Alto, CA) **(**Figure S3**)**.

Fabrication of tough cryogels

Tough cryogels were fabricated using a combination of covalent and ionic crosslinking of alginate. First, covalently crosslinked-only cryogels were formed.[14] Briefly, 1.5% (w/v) MA-alginate solution in deionized water was mixed with polymerization initiators TEMED (0.5% w/v) and APS (0.25% w/v). The mixture was quickly added to Teflon molds (5 mm diameter, 1 mm height) which were placed at −20°C overnight while crosslinking occurred. Cryogels were thawed and then soaked in 200 mM calcium chloride to form ionic crosslinking with calcium ions. They were soaked for different durations to vary calcium concentration in the gels. To quantify calcium concentrations in the gels, the gels were washed in a 25 mM HEPES buffer supplemented by 2 mM $CaCl_2$ and 140 mM NaCl for 1 min under gentle stirring to remove excess calcium ions from the pores. Gels were then digested in 1 mL 10 U/mL alginate lyase on a shaker by incubating overnight at RT. Samples were quantified using a calcium assay kit (BioVision, Milpitas, CA). When used, GM-CSF, CpG-ODN and OVA, were mixed in the MA-alginate polymer solution prior to cryogelation. Cell-adhesive tough cryogels were fabricated by adding 0.8% (w/v) of ACRL-PEG-RGD to the MA-alginate solution as a comonomer prior to cryogelation.

Physical characterization of cryogels

To determine whether cryogels could undergo needle injection without sustaining damage, cryogels (5 mm in diameter and 1 mm in thickness) were injected with ~250 μL of deionized water or a $CaCl_2$ solution through a 16G or 18G needle. They were visually inspected and classified as either intact or damaged. A damaged gel is defined as a gel with any visible macroscopic fracture.

HFUS imaging was performed to determine the effects of cryogel formulation and needle injection type (16 v. 18 gauge) on the ability of cryogels to maintain their original morphology *in vivo* post-injection. Cryogels were injected in ~250 μL of PBS using a 16 or 18G needle subcutaneously into the backs of female, 6-8 week-old BALBc/J mice (n = 3). Immediately following injection, sagittal B-mode images were acquired throughout the cryogel width (spacing 0.5mm) (Vevo 770 scanner; 35 MHz transducer (RMV712); axial resolution: 50μm, lateral resolution: 140μm, field of view: 15mm); VisualSonics, Toronto, Canada). Cryogel sections were segmented from each image slice in MATLAB (vR2017a; Mathworks, Natick, MA) and the three centermost images were evaluated for circularity ($C = 4 \times \pi \times \text{Area} / \text{perimeter}^2$; range: 0→1 (circular)) and thickness as metrics of cryogel morphology. Cryogels were then explanted for inspection.

SEM was used to examine cryogels' porous structure. Prior to imaging, cryogels were serially dehydrated in increasing concentrations of ethanol (30, 50, 70, 90, and 100%) for 20 min each, incubated in HMDS for 10 min, and dried in a vacuum chamber for 1 h.[41] Dried samples were mounted on aluminum pin mounts using conductive carbon tape, sputter-coated with gold, and then imaged using a Tescan Vega III SEM.

The bulk physical dimensions (diameter and thickness) were measured using a caliper before and after injections through a 16G or 18G needle.

For confocal microscopy imaging, cryogels were first covalently labeled with a Cy5 dye via a carbodiimide crosslinker chemistry. Briefly, cryogels were submerged in a 0.1 M MES buffer (pH ~6.5) with NHS (7.8 mg/mL) and EDC (16.8 mg/mL), at 1 gel/mL for 10 min, followed by addition of Cy5-amine (6.9 μg/mL) to the reaction mixture. The reaction was incubated during gentle shaking for 2 h at RT in the dark, and then cryogels were washed in DI water to remove excess fluorescent dye. Cy5-labeled cryogels were then imaged in HBSS using an Upright Zeiss LSM710 NLO microscope. When tough cryogels were imaged, $CaCl_2$ (2 mM) was added to HBSS to prevent calcium ions in the gel from leaching out. Two cross-sections 200 μm apart were imaged per cryogel. The cryogel images were analyzed by the ImageJ software (Fiji Java 6 20170530 version) using the Bond plugin.[42] The pore spaces were fitted with the maximal spheres that could fit in the space. The diameters of these maximal spheres inform the dimensions of the pore space locally.[43–45]

Cryogels (8 mm in diameter and 6 mm in thickness) were characterized for Young's Modulus, interconnected porosity, and swelling ratio. The Young's Moduli of the cryogels were found using compression tests on an Instron with a 20%/min strain rate.[46] Interconnected porosity and swelling ratio were determined using the wicking method.[14] Interconnected porosity (P) was calculated as $P = m_p / m_s \times 100\%$, where m_p is the mass of water wicked away (calculated by taking the mass difference between the fully hydrated and dehydrated sample), and m_s is the mass of the fully hydrated sample. Swelling ratio (Q) was calculated as $Q = m_s / m_d$, where m_d is the mass of the dried sample.

Generation of BMDC and DC activation in vitro by tough cryogels

Bone marrow-derived DCs (BMDCs) were generated according to standard protocols.[47–48] Briefly, hindlimbs of 6-8 week-old female BALB/cJ mice were harvested. The femurs and tibias were flushed by culture media (RPMI 1640 media supplemented with 10% heat-inactivated FBS, 1% penicillin/streptomycin, 50 μM β-mercaptoethanol, and 20 ng/mL GM-CSF) to isolate bone marrow cells, which were then cultured for 7 days. BMDCs cultured between 7 and 10 days were collected and used for experiments. BMDCs were cultured in tough or covalently crosslinked-only cryogels to determine whether calcium in the tough cryogel can activate DCs. To study whether CpG-ODN-delivering tough cryogels could activate DCs long term, tough cryogels delivering 35 μg CpG-ODN were placed in 1 mL of a solution of 1% bovine serum albumin (BSA) in PBS, and the release buffer was collected and replaced with fresh buffer at every time point. Released CpG-ODN was quantified by the Quant-it™ OliGreen® ssDNA Assay Kit. After releasing CpG-ODN *in vitro* for up to 2 weeks, the tough cryogels were then incubated on a monolayer of 3×10^5 BMDCs overnight. Viability of the DCs and upregulation of DC activation markers were assessed by flow cytometry (FACS; BD LSR Fortessa, San Jose, CA) using APC-Cy7-conjugated fixable live/dead stain and APC-conjugated CD11c, FITC-conjugated CD86, and PE-Cy7-conjugated MHC II stains. FACS analyses were compensated.

Immune cell recruitment to tough cryogels

Gels containing 1.5 μg GM-CSF were placed in 1 mL of a solution of 1% bovine serum albumin (BSA) in PBS, and the release buffer was collected and replaced with fresh buffer at every time point. Released GM-CSF was quantified by ELISA. Two tough cryogels

containing no bioactives (blank) or 1.5 μg of GM-CSF were injected subcutaneously via a 16G needle in the lower flanks near the inguinal LNs of 6-8 week-old female BALB/cJ mice. On day 7, the scaffolds were explanted and incubated in 250 U/mL collagenase type IV under agitation at 37°C for 30 min. The resulting cell suspensions were filtered through a 40 μm cell strainer to isolate the cells from debris. Total cell count was performed by Countess II automated cell counter (Thermo Fisher Scientific). To identify immune cells and determine their viability and activation states, cells were stained with fluorescently-labeled primary antibodies and analyzed by FACS. APC-Cy7-conjugated fixable live/dead stain was used to determine viability. APC-conjugated CD11c and PE-Cy7-conjugated CD11b stains were used to identify DCs. FITC-conjugated Ly6G and PE-Cy7-conjugated CD11b stains were used to identify neutrophils. PE-conjugated F4/80 and PE-Cy7-conjugated CD11b stains were used to identify macrophages. FACS analyses were compensated, and cells were gated according to positive APC, FITC, PE, and PE-Cy7 using isotype controls. Based on the total cell count and the percentage of DCs, neutrophils and macrophages determined by FACS, the number of each cell type in the scaffold was calculated.

Preparation of tough cryogel OVA vaccines and vaccination

GM-CSF, CpG-ODN and OVA, were mixed in the MA-alginate polymer solution prior to cryogelation, with a final dose of 1.5 μg of GM-CSF, 35 μg of CpG-ODN and 150 ug of OVA encapsulated per tough cryogel. Two of these tough cryogels were injected in ~250 μL of PBS by a 16G needle subcutaneously into lower flanks near the inguinal LNs of female, 6-8 week-old C57BL/6J mice (n = 5). Two blank tough cryogels were injected into each mouse as a control (n = 5).

Detection of OVA-specific cytotoxic T-lymphocyte responses

Blood was drawn from the mice 8 days after vaccination, and red blood cells were lysed by using the ACK lysis buffer. Half of the remaining blood cells were first stained with APC-conjugatedH-2Kb-SIINFEKL tetramer and subsequently stained with the FITC-conjugated CD8 stain (eBioscience) for FACS analysis. The other half of the cells were co-incubated with 7 ug/mL of $OVA_{257-264}$ SIINFEKL OVA CD8 epitope in a 96-well U-bottomed plate for 1.5 h at 37°C. 50 uL of 1× GolgiStop™ (BD Biosciences) was added to each well and the cell were incubated for another 4 h at 37°C. The samples were stained with APC-Cy7-conjugated fixable live/dead stain and the FITC-conjugated CD8 stain (eBioscience). Then, the samples were incubated in Cytomix/Cytoperm (BD Biosciences) for 20 min at 4°C, washed in Perm Wash buffer and stained with APC-conjugated IFN-γ stain for FACS analysis. FACS analyses were compensated.

Detection of serum anti-OVA antibodies

Serum anti-OVA antibody titer was quantified by ELISA. Briefly, blood was drawn from C57BL/6J mice 4 weeks after vaccination, and sera were isolated from blood by centrifugation at 2,200 g for 10 min. ELISA plates were coated with 10 ug/mL OVA in PBS in 4°C overnight during gentle mixing. ELISA was performed following standard, established procedure. Anti-OVA titer is defined as the lowest serum dilution where the ELISA OD value was 0.2.

Preparation of tough cryogel breast cancer vaccines and vaccination

GM-CSF and CpG-ODN were mixed in the MA-alginate/ACRL-PEG-RGD polymer solution prior to cryogelation, with a final dose of 1.5 μg of GM-CSF and 35 μg of CpG-ODN encapsulated per tough cryogel. The tough cryogels were mechanically compressed to partially squeeze out water in the pores before seeding irradiated tumor cells as the antigen. DD breast cancer cells were irradiated at a dose of 3,500 rads from a ^{137}C source. Twenty microliters of cell suspensions at 1×10^7 cells/mL in complete RPMI 1640 cell culture media (supplemented with 10% FBS and 1% penicillin/streptomycin) were pipetted into tough cryogels (total of 2×10^5 cells/gel) and were incubated at 37°C, 5% CO_2 for 6 h to allow for cell adhesion.[12]

Two tough cryogels loaded with 1.5 μg of GM-CSF, 35 μg of CpG-ODN, and 2×10^5 irradiated DD cells per gel were injected in ~250 μL of PBS by a 16G needle subcutaneously into lower flanks of female 6-8 week-old BALB/cJ mice (n = 5). As a control, two blank tough cryogels were injected into each mouse (n = 7). Blood was drawn from the mice periodically to assess anti-HER2/neu antibody level in sera. Thirty days after vaccination, the mice were challenged by 1×10^5 DD breast cancer cells injected subcutaneously in the back of the neck. Tumor growth and mouse survival were monitored. Tumors were assumed to be in an oval shape and tumor areas were calculated by the equation length × width × π / 4. Mice were euthanized for humane reasons when the longest dimension of the tumor was greater than 20 mm, total tumor area was greater than 200 mm^2, or severe ulceration or bleeding occurred.

Detection of serum anti-HER2/neu antibodies

The method to detect anti-HER2/neu antibodies in sera was adapted from a previous protocol.[49] Blood was drawn from BALB/cJ mice, and sera were isolated from blood by centrifugation at 2,200 g for 10 min. Sera were diluted 100-fold and incubated with 100,000 CT26 cells or HER2/neu-overexpressing CT26 cells for 20 min on ice. The cells were then stained with 200-fold diluted PE-conjugated anti-mouse pan-IgG secondary antibody (Jackson ImmunoResearch) for 20 min on ice. The cells were analyzed by FACS, and the mean fluorescence intensity ratio between CT26 and HER2/neu-overexpressing CT26 cells was calculated.

Animal protocol

All animal studies were performed in accordance with National Institutes of Health guidelines, and with the approval of Harvard University's Institutional Animal Care and Use Committee.

Statistical analysis

All values presented in this manuscript were expressed as mean ± s.d. Statistical analyses were performed using GraphPad Prism or Microsoft Excel unless otherwise specified. Data from the injection tests were analyzed by binomial tests. Two-way ANOVAs with post hoc Student's t-tests with Bonferroni corrections were used to evaluate the effects of cryogel formulation and needle gauge injection type on cryogel circularity and thickness (SPSS, v24, Armonk, NY). Mann-Whitney tests were used to analyze anti-OVA antibody titers. The

survival data were analyzed by the Log-rank Mantel-Cox test. For other data, sample variance was first tested using the F-test to determine whether samples had equal variance. Samples with equal variance were analyzed by a two-tailed Student's t-test. Samples with unequal variance were analyzed by a two-tailed Welch's t-test. Differences with $p < 0.05$ were considered statistically significant.

Supplementary Material

Refer to Web version on PubMed Central for supplementary material.

Acknowledgement

This work is supported by the National Institutes of Health (R01 EB015498, R01 DK098055, F32AG057135), National Science Foundation Graduate Research Fellowship Program, Howard Hughes Medical Institute International Student Research Fellowship, and the Wyss Institute for Biologically Inspired Engineering. The authors would like to thank Dr. James Weaver for his help with SEM imaging, Dr. Adam Celiz for his help with NMR analysis, and Dr. Angelo Mao and Mr. Brian Kwee for his help with confocal microscopy imaging and analysis.

References

[1]. Curigliano G, Locatelli M, Fumagalli L, Goldhirsch A, Breast 2009, 18 Suppl 3, S51. [PubMed: 19914543]

[2]. Wong KK, Li WA, Mooney DJ, Dranoff G, Adv Immunol 2016, 130, 191. [PubMed: 26923002]

[3]. Yaguchi T, Sumimoto H, Kudo-Saito C, Tsukamoto N, Ueda R, Iwata-Kajihara T, Nishio H, Kawamura N, Kawakami Y, Int J Hematol 2011, 93, 294. [PubMed: 21374075]

[4]. Mellman I, Coukos G, Dranoff G, Nature 2011, 480, 480. [PubMed: 22193102]

[5]. Nayar S, Dasgupta P, Galustian C, Oncoimmunology 2015, 4, e1002720. [PubMed: 26155387]

[6]. Yee C, J Transl Med 2005, 3, 17. [PubMed: 15860133]

[7]. Li WA, Mooney DJ, Curr Opin Immunol 2013, 25, 238. [PubMed: 23337254]

[8]. Mehta NK, Moynihan KD, Irvine DJ, Cancer Immunol Res 2015, 3, 836. [PubMed: 26156157]

[9]. Koshy ST, Mooney DJ, Curr Opin Biotechnol 2016, 40, 1. [PubMed: 26896596]

[10]. Ali OA, Emerich D, Dranoff G, Mooney DJ, Sci Transl Med 2009, 1, 8ra19.

[11]. Kim J, Li WA, Choi Y, Lewin SA, Verbeke CS, Dranoff G, Mooney DJ, Nat Biotechnol 2015, 33, 64. [PubMed: 25485616]

[12]. Bencherif SA, Warren Sands R, Ali OA, Li WA, Lewin SA, Braschler TM, Shih TY, Verbeke CS, Bhatta D, Dranoff G, Mooney DJ, Nat Commun 2015, 6, 7556. [PubMed: 26265369]

[13]. Dana-Farber Cancer Institute, Dendritic Cell Activating Scaffold in Melanoma, http://clinicaltrials.gov/ct2/show/NCT01753089?term=NCT01753089&rank=1, accessed: December 13, 2017.

[14]. Bencherif SA, Sands RW, Bhatta D, Arany P, Verbeke CS, Edwards DA, Mooney DJ, Proc Natl Acad Sci U S A 2012, 109, 19590. [PubMed: 23150549]

[15]. Guvendiren M, Lu HD, Burdick JA, Soft Matter 2012, 8, 260.

[16]. Sun JY, Zhao X, Illeperuma WR, Chaudhuri O, Oh KH, Mooney DJ, Vlassak JJ, Suo Z, Nature 2012, 489, 133. [PubMed: 22955625]

[17]. Lee KY, Mooney DJ, Prog Polym Sci 2012, 37, 106. [PubMed: 22125349]

[18]. Vaeth M, Eckstein M, Shaw PJ, Kozhaya L, Yang J, Berberich-Siebelt F, Clancy R, Unutmaz D, Feske S, Immunity 2016, 44, 1350. [PubMed: 27261277]

[19]. Rossol M, Pierer M, Raulien N, Quandt D, Meusch U, Rothe K, Schubert K, Schoneberg T, Schaefer M, Krugel U, Smajilovic S, Brauner-Osborne H, Baerwald C, Wagner U, Nat Commun 2012, 3, 1329. [PubMed: 23271661]

[20]. Tayalia P, Mazur E, Mooney DJ, Biomaterials 2011, 32, 2634. [PubMed: 21237507]

[21]. Augst AD, Kong HJ, Mooney DJ, Macromol Biosci 2006, 6, 623. [PubMed: 16881042]

[22]. Beduer A, Braschler T, Peric O, Fantner GE, Mosser S, Fraering PC, Bencherif S, Mooney DJ, Renaud P, Adv Healthc Mater 2015, 4, 301. [PubMed: 25178838]

[23]. Sun G, Li Z, Liang R, Weng LT, Zhang L, Nat Commun 2016, 7, 12095. [PubMed: 27352822]

[24]. Liu R, Liang S, Tang X-Z, Yan D, Li X, Yu Z-Z, J. Mater. Chem 2012, 22, 14160.

[25]. Collins AM, Immunol Cell Biol 2016, 94, 949. [PubMed: 27502143]

[26]. Lee GS, Subramanian N, Kim AI, Aksentijevich I, Goldbach-Mansky R, Sacks DB, Germain RN, Kastner DL, Chae JJ, Nature 2012, 492, 123. [PubMed: 23143333]

[27]. Murakami T, Ockinger J, Yu J, Byles V, McColl A, Hofer AM, Horng T, Proc Natl Acad Sci U S A 2012, 109, 11282. [PubMed: 22733741]

[28]. Jin C, Frayssinet P, Pelker R, Cwirka D, Hu B, Vignery A, Eisenbarth SC, Flavell RA, Proc Natl Acad Sci U S A 2011, 108, 14867. [PubMed: 21856950]

[29]. Baroja-Mazo A, Martin-Sanchez F, Gomez AI, Martinez CM, Amores-Iniesta J, Compan V, Barbera-Cremades M, Yague J, Ruiz-Ortiz E, Anton J, Bujan S, Couillin I, Brough D, Arostegui JI, Pelegrin P, Nat Immunol 2014, 15, 738. [PubMed: 24952504]

[30]. Chan G, Mooney DJ, Acta Biomater 2013, 9, 9281. [PubMed: 23938198]

[31]. Kolaczkowska E, Kubes P, Nat Rev Immunol 2013, 13, 159. [PubMed: 23435331]

[32]. Gulley JL, Madan RA, Schlom J, Curr Oncol 2011, 18, e150. [PubMed: 21655153]

[33]. Ogi C, Aruga A, Hum Vaccin Immunother 2013, 9, 1049. [PubMed: 23454867]

[34]. Hartmann LC, Schaid DJ, Woods JE, Crotty TP, Myers JL, Arnold PG, Petty PM, Sellers TA, Johnson JL, McDonnell SK, Frost MH, Jenkins RB, N Engl J Med 1999, 340, 77. [PubMed: 9887158]

[35]. Rebbeck TR, Friebel T, Lynch HT, Neuhausen SL, van ’t Veer L, Garber JE, Evans GR, Narod SA, Isaacs C, Matloff E, Daly MB, Olopade OI, Weber BL, J Clin Oncol 2004, 22, 1055. [PubMed: 14981104]

[36]. Domchek SM, Friebel TM, Singer CF, Evans DG, Lynch HT, Isaacs C, Garber JE, Neuhausen SL, Matloff E, Eeles R, Pichert G, Van t’veer L, Tung N, Weitzel JN, Couch FJ, Rubinstein WS, Ganz PA, Daly MB, Olopade OI, Tomlinson G, Schildkraut J, Blum JL, Rebbeck TR, JAMA 2010, 304, 967. [PubMed: 20810374]

[37]. Ali OA, Huebsch N, Cao L, Dranoff G, Mooney DJ, Nat Mater 2009, 8, 151. [PubMed: 19136947]

[38]. Elpek KG, Cremasco V, Shen H, Harvey CJ, Wucherpfennig KW, Goldstein DR, Monach PA, Turley SJ, Cancer Immunol Res 2014, 2, 655. [PubMed: 24801837]

[39]. Draganov D, Gopalakrishna-Pillai S, Chen YR, Zuckerman N, Moeller S, Wang C, Ann D, Lee PP, Sci Rep 2015, 5, 16222. [PubMed: 26552848]

[40]. Bencherif SA, Srinivasan A, Horkay F, Hollinger JO, Matyjaszewski K, Washburn NR, Biomaterials 2008, 29, 1739. [PubMed: 18234331]

[41]. Koshy ST, Ferrante TC, Lewin SA, Mooney DJ, Biomaterials 2014, 35, 2477. [PubMed: 24345735]

[42]. Doube M, Klosowski MM, Arganda-Carreras I, Cordelieres FP, Dougherty RP, Jackson JS, Schmid B, Hutchinson JR, Shefelbine SJ, Bone 2010, 47, 1076. [PubMed: 20817052]

[43]. Hildebrand T, Rüegsegger P, J. Microsc 1997, 185, 67.

[44]. Hildebrand T, Laib A, Muller R, Dequeker J, Ruegsegger P, J Bone Miner Res 1999, 14, 1167. [PubMed: 10404017]

[45]. Peters OA, Laib A, Gohring TN, Barbakow F, J Endod 2001, 27, 1. [PubMed: 11487156]

[46]. Cezar CA, Kennedy SM, Mehta M, Weaver JC, Gu L, Vandenburgh H, Mooney DJ, Adv Healthc Mater 2014, 3, 1869. [PubMed: 24862232]

[47]. Faulkner L, Buchan G, Baird M, Immunology 2000, 99, 523. [PubMed: 10792499]

[48]. Bhattacharya P, Gopisetty A, Ganesh BB, Sheng JR, Prabhakar BS, J Leukoc Biol 2011, 89, 235. [PubMed: 21048215]

[49]. Dela Cruz JS, Trinh KR, Morrison SL, Penichet ML, J Immunol 2000, 165, 5112. [PubMed: 11046042]

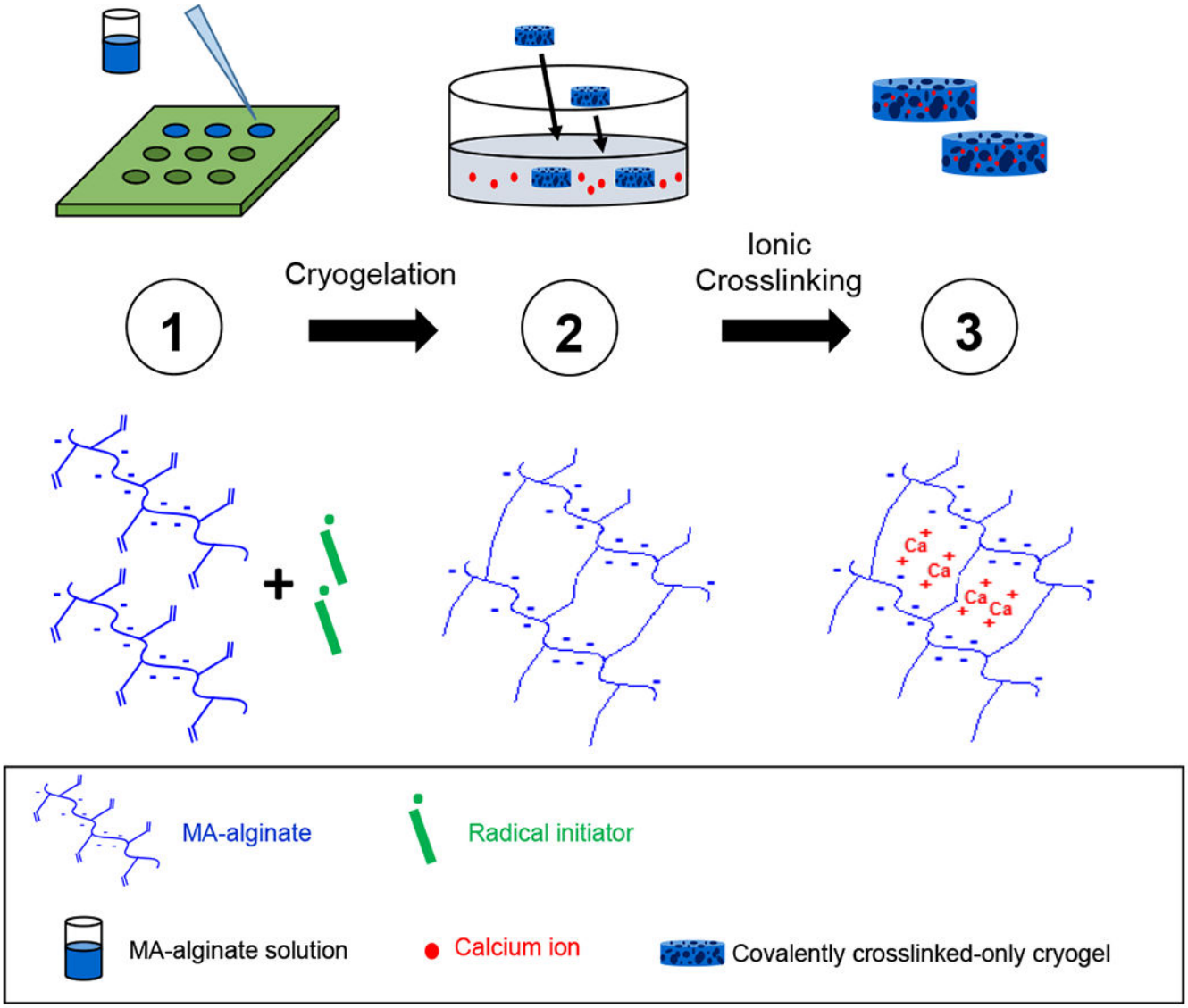

Figure 1. Fabrication of MA-alginate tough cryogels.

(Top row) Fabricating MA-alginate tough cryogels. Step 1: MA-alginate solution mixed with radical initiators (APS/TEMED) is quickly added to a Teflon mold and placed at −20°C overnight to form macroporous covalently crosslinked-only cryogels; Step 2: Covalently crosslinked cryogels are placed in a $CaCl_2$ bath to form ionic crosslinking; Step 3: MA-alginate tough cryogels with both covalent and ionic crosslinking result. (Bottom row) Crosslinking state of MA-alginate polymer chains at each step. Step 1: Uncrosslinked free polymer chains; Step 2: covalently crosslinked cryogels; Step 3: covalently and ionically crosslinked tough cryogels.

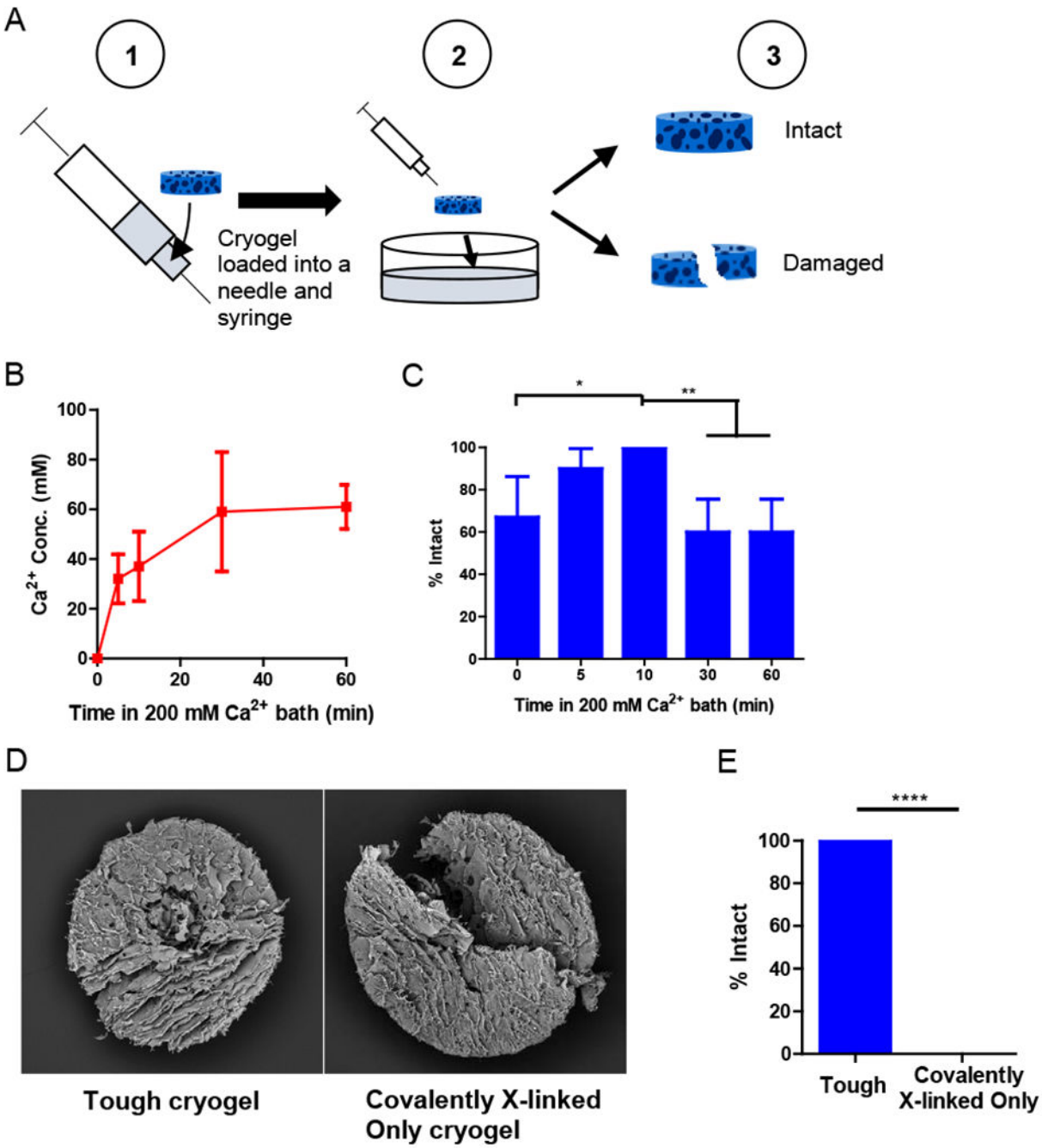

Figure 2. Tough cryogels remain intact after needle injection *in vitro*.

(A) Process of injection testing. A cryogel is loaded into a needle and syringe ① and then injected into a bath ②. The gel is visually inspected to determine whether it is intact or damaged ③. (B) Calcium concentrations in cryogels after different durations of soaking in a 200 mM calcium bath. $n = 4$. (C) Percentage of cryogels that were intact (% Intact) after needle injection through a 16G needle, as a function of soaking duration in a 200 mM calcium bath. $n = 6$-10. (D) Scanning electron microscopy images of tough cryogels (10 min soaking in a 200 mM calcium bath) (left) and covalently crosslinked-only cryogels (right)

after injection via an 18G needle. (E) Percentage of intact tough cryogels (10 min soaking in a 200 mM calcium bath) and covalently crosslinked-only cryogels after injection via an 18G needle. Some error bars are too small to be seen. $n = 9$. Values presented were expressed as mean ± s.d. Data were analyzed by a binomial test.* $p < 0.05$, ** $p < 0.01$, **** $p < 0.0001$.

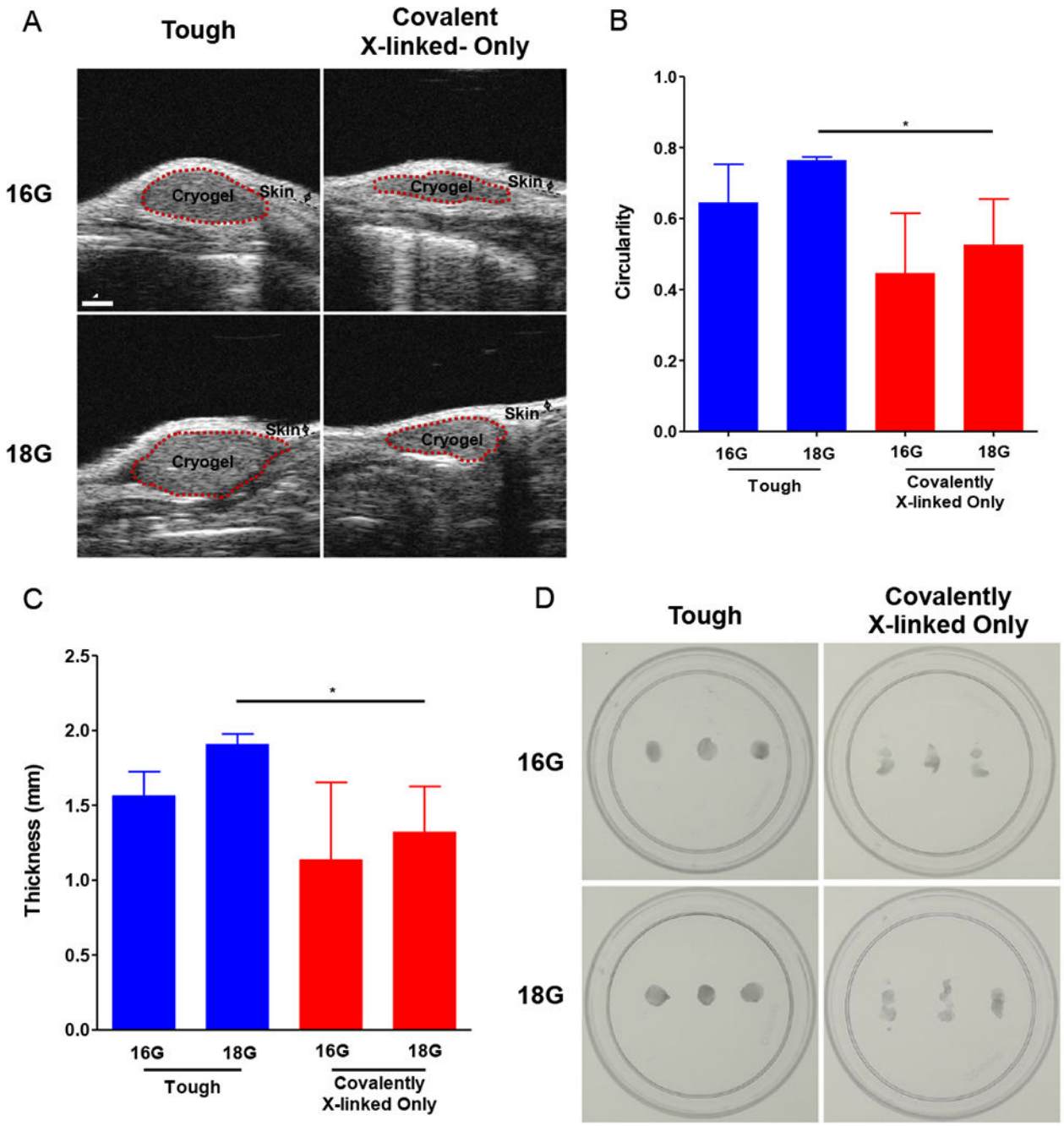

Figure 3. Tough cryogels remain intact after subcutaneous injection into the backs of mice.

(A) Representative sagittal B-mode high frequency ultrasound *in vivo* images of cryogels injected via al6G or 18G needle. Circularity (B) and gel thickness (C) as a function of cryogel formulation (tough v. covalently crosslinked-only) and needle injection type (16 v. 18G). (D) Images of cryogels after explantation. $n = 3$. Values presented were expressed as mean ± s.d. Data were analyzed by two-way ANOVAs with post hoc Student's t-tests with Bonferroni corrections * $p < 0.05$.

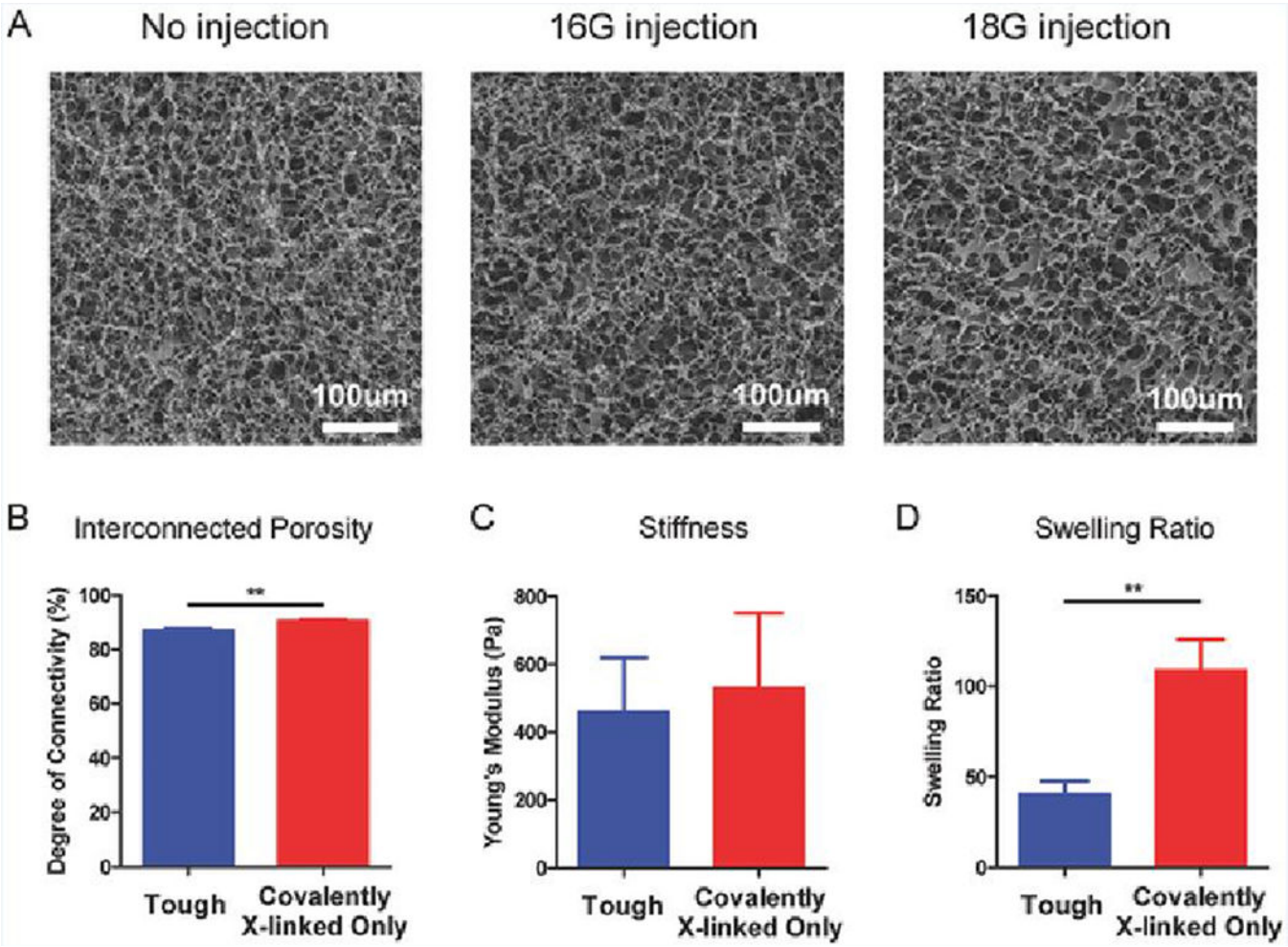

Figure 4. Physical characterization of tough cryogels.

(A) Representative scanning electron microscopy images of tough cryogels without injection (left) and after 16G (middle) or 18G (right) needle injection. Interconnected porosity (B), stiffness (C), and swelling ratio (D) of tough and covalently crosslinked-only cryogels. n = 3. Values presented were expressed as mean ± s.d. Data were analyzed by a two-tailed Student's t-test. ** $p < 0.01$

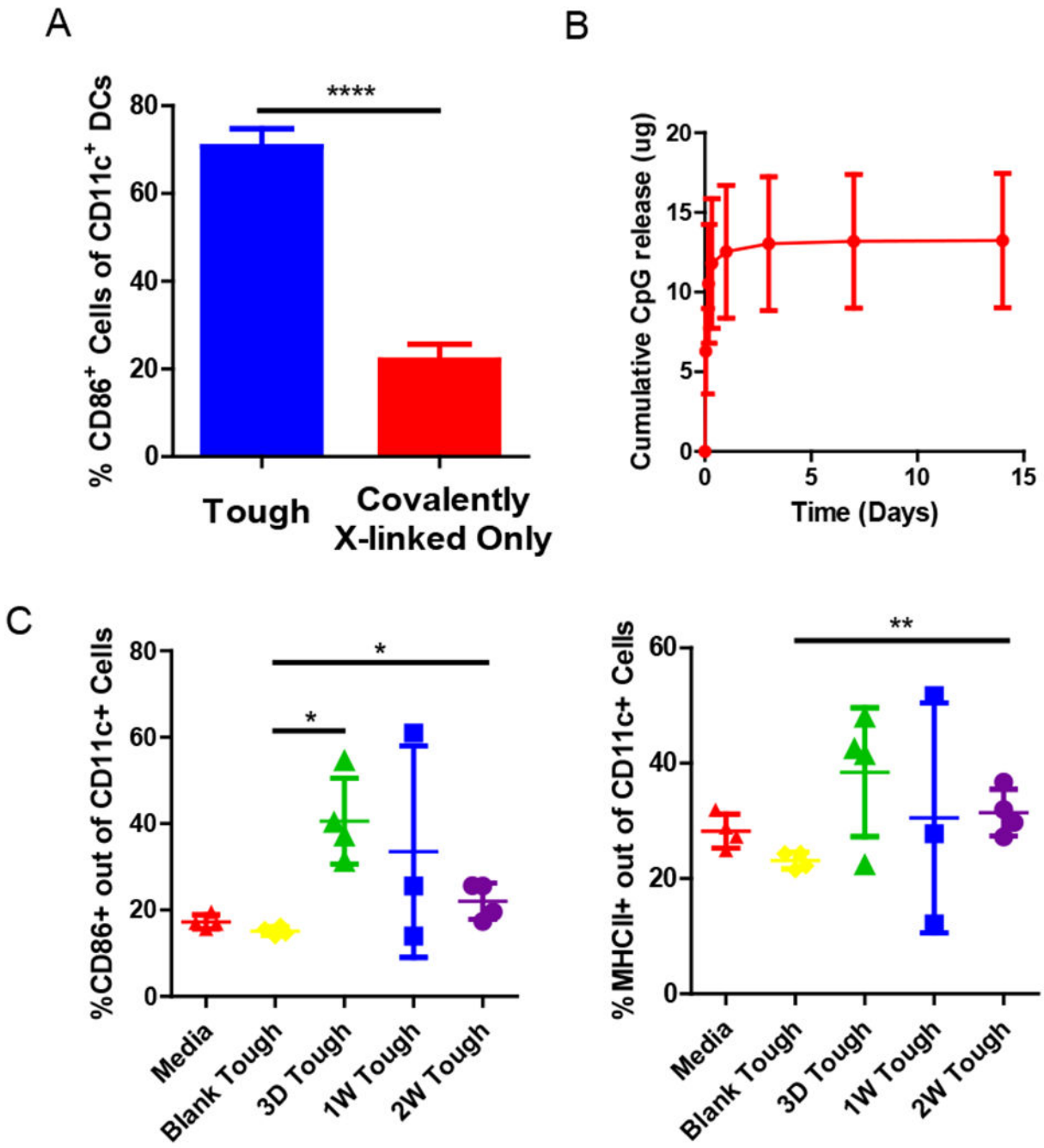

Figure 5. ***In vitro*** **BMDC activation by tough cryogels.**

(A) Fractions of $CD86^+$ $CD11c^+$ DCs after culture in tough and covalently crosslinked-only cryogels, as analyzed by flow cytometry. (B) Cumulative release of CpG-ODN from tough cryogels. (C) Fractions of $CD86^+$ (left) and MHC II^+ (right) $CD11c^+$ DCs after culture in media alone, tough cryogels containing no CpG-ODN (Blank Tough), or tough cryogels delivering CpG-ODN after cryogels were previously allowed to release CpG-ODN for 3 days, 1 week or 2 weeks (3D Tough, 1W Tough and 2W Tough) prior to exposure to DCs. *n*

= 4. Values presented were expressed as mean ± s.d. Data were analyzed by a two-tailed Student's t-test or Welch's t-test. * $p < 0.05$, ** $p < 0.01$, **** $p < 0.0001$.

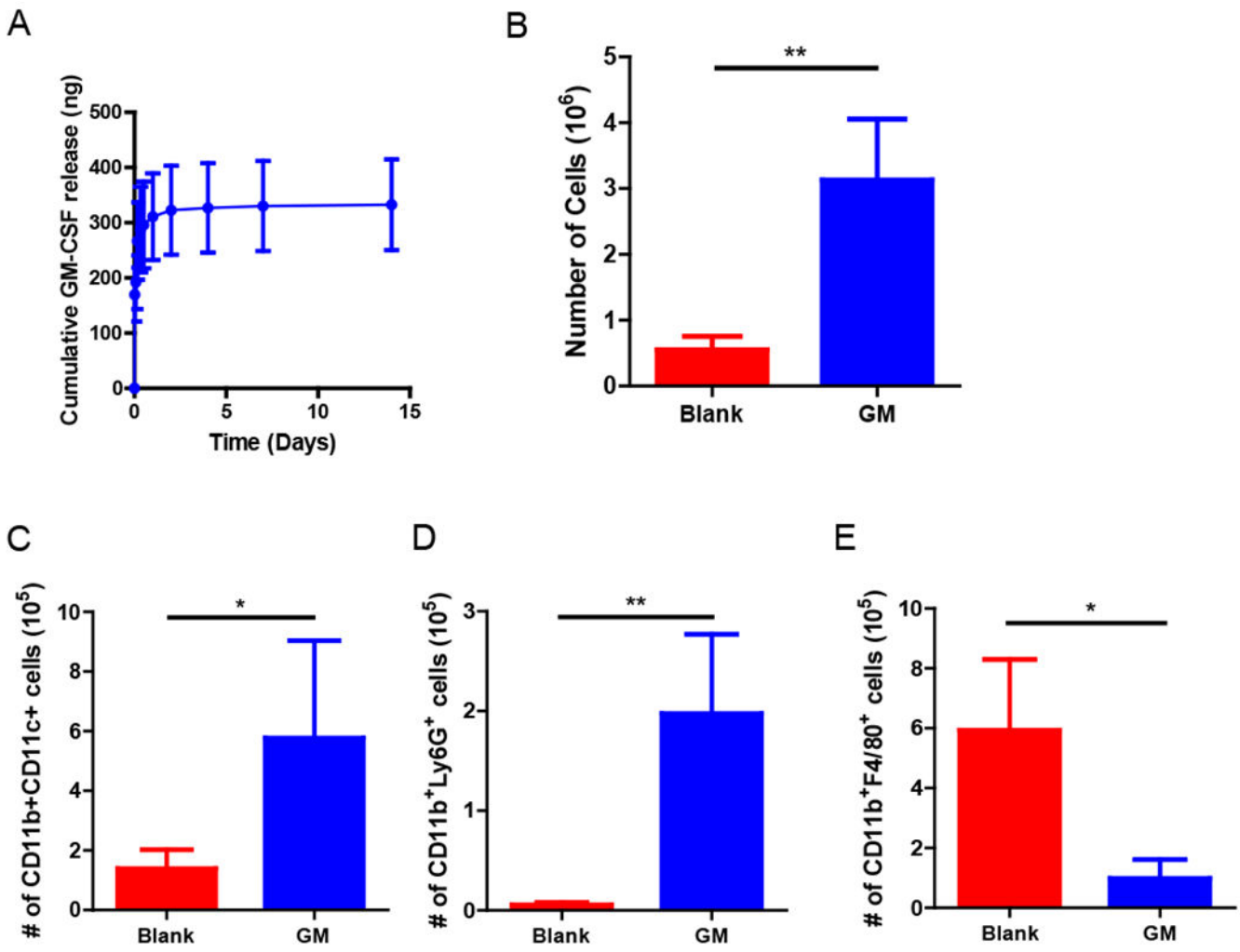

Figure 6. ***In vivo*** **immune cell recruitment by tough cryogels delivering GM-CSF.**

(A) Cumulative release of GM-CSF from tough cryogels. (B) Total number of cells present in blank tough and GM-CSF-delivering tough cryogels 7 days after implantation. Quantification of (C) $CD11b^+$ $CD11c^+$ DCs (D) $CD11b^+Ly6G^+$ neutrophils and (E) $CD11b^+F4/80^+$ macrophages in cryogels. n = 5-6. Values presented were expressed as mean ± s.d. Data were analyzed by a two-tailed Student's t-test or Welch's t-test. * $p < 0.05$, ** $p < 0.01$.

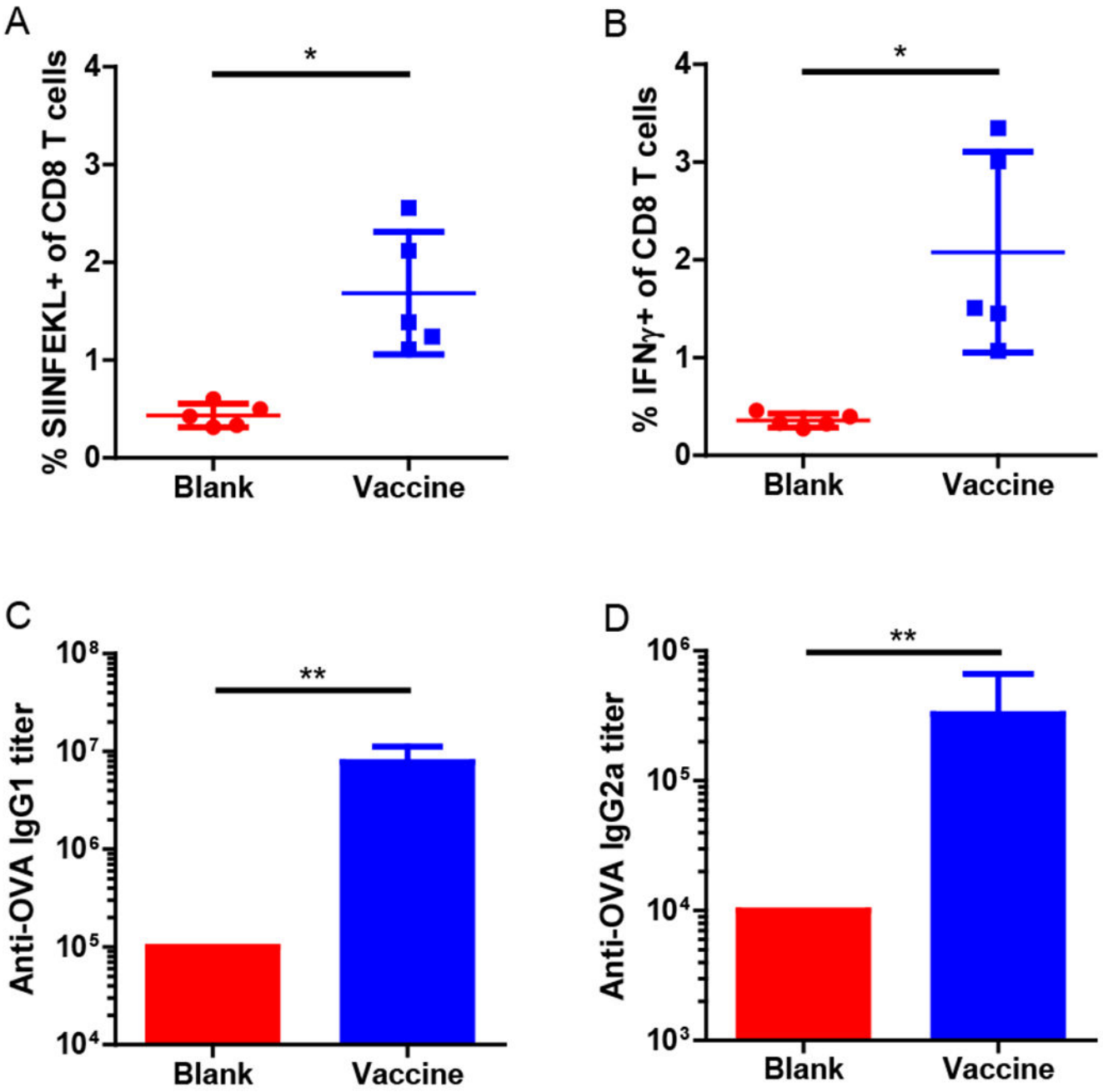

Figure 7. ***In vivo*** **antigen-specific immune responses induced by the tough cryogel vaccine.**
Fractions of (A) SIFNFEKL^{+} and (B) IFN-γ^{+} cells among blood CD8 T cells in mice vaccinated with tough cryogel vaccines compared to mice treated with blank tough cryogels. Titers of (C) IgGl and (D) IgG2a anti-OVA antibodies in sera of mice vaccinated with tough cryogel vaccines compared to mice treated with blank tough cryogels. The antibody titers of the blank group presented here are the lowest serum dilution. Some error bars are too small to be seen. $n = 5$. Values presented were expressed as mean ± s.d. Data were analyzed by a two-tailed Welch's t-test for the T cell response experiment and by a Mann-Whitney test for the antibody titer experiment. * $p < 0.05$, ** $p < 0.01$.

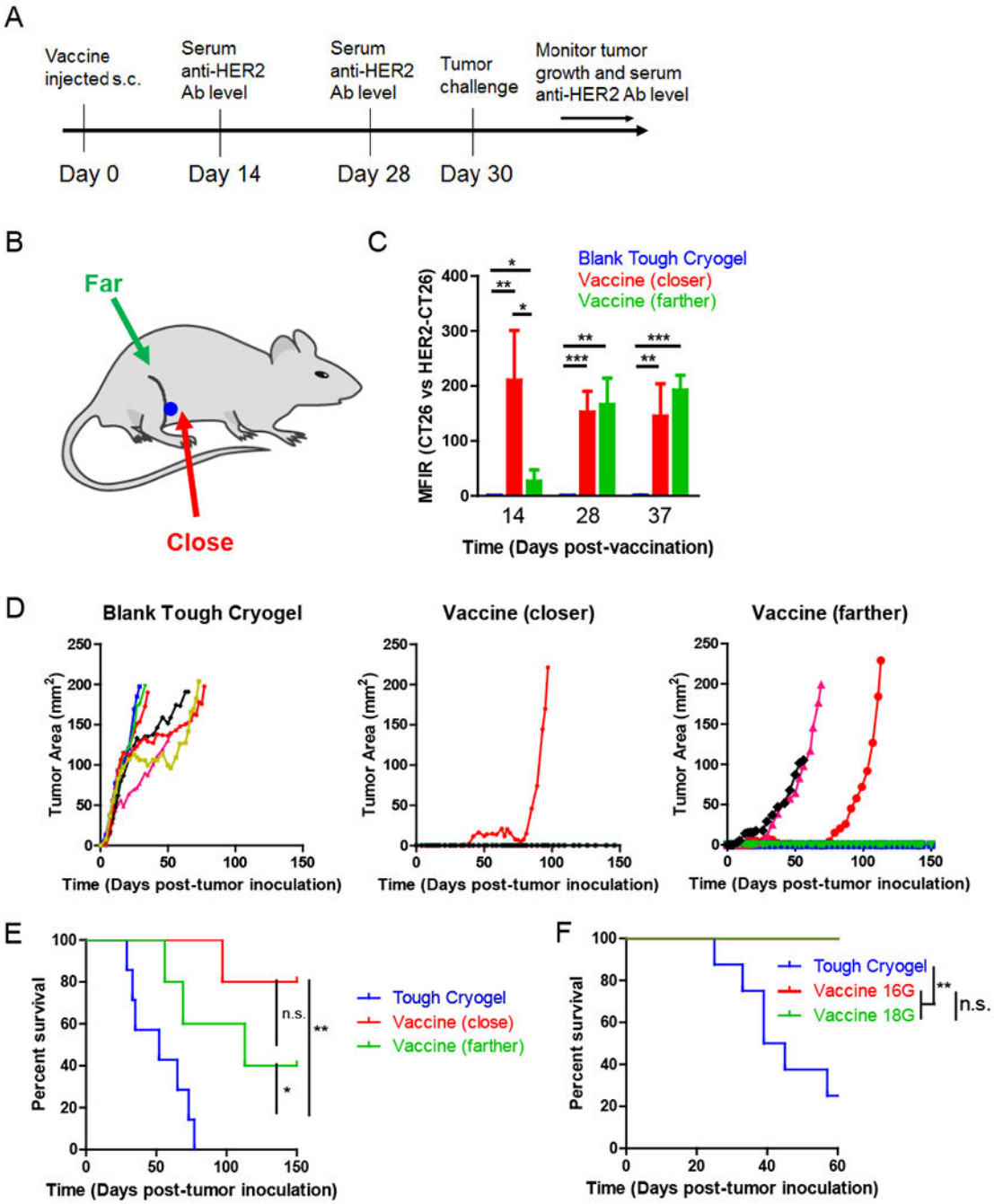

Figure 8. Prophylactic efficacy of the tough cryogel vaccine.

(A) Outline of the prophylactic vaccination study. (B) Locations of injected tough cryogels. A 16G needle was used for injection unless specified otherwise. (C) Serum anti-HER2/neu antibody levels in mice vaccinated by the tough cryogel vaccine. (D) Tumor growth curves of individual mice vaccinated by blank cryogels ($n = 7$; left) or tough cryogel vaccines injected close ($n = 5$; middle) or far from the draining lymph nodes ($n = 5$; right). (E) Survival rates of mice challenged by HER2/neu-expressing DD breast cancer cells after vaccination by blank tough cryogels or tough cryogel vaccines injected close or far from the

draining lymph nodes. (F) Survival rates of mice challenged by HER2/neu-expressing DD breast cancer cells after vaccination by blank tough cryogels or tough cryogel vaccines injected via a 16G or 18G needle. $n = 8$ (vaccines injected with both gauge needles led to 100% survival). Vaccines were injected in close proximity to the dLN. Values presented were expressed as mean ± s.d. Data were analyzed by a two-tailed Student's t-test or Welch's t-test for the antibody MFIR experiment, and by a Log-rank Mantel-Cox test for the survival experiments. * $p < 0.05$, ** $p < 0.01$, *** $p < 0.001$, n.s. not significant.